Chapter 2
Interferences with Massive Particles

2.1 The De Broglie Wave-Particle Duality

2.1.1 The Concept of Wave-Particle Duality

Parallel to the introduction by Einstein of the concept of quanta for light, Niels Bohr showed that the quanta idea could be extended to atoms [1]. Coming back to the model of an atom introduced by Ernest Rutherford, where the atom consisted of a "positively charged nucleus surrounded by a system of electrons kept together by attractive forces from the nucleus", Bohr pointed out "difficulties of a serious nature arising from the apparent instability of the system of electrons". It is well established that, when a charged particle accelerates, radiation is emitted. Thus, the electron will lose energy and follow orbits of smaller and smaller sizes. To avoid these difficulties, Bohr referred to Planck's theory and forced the orbits to be stable, with the electrons emitting no radiation. An atom was now considered as a microscopic solar system. At such a small scale, "the electrons and other massive corpuscles do not follow [...] classical mechanics laws, but can have defined motion states [...] that satisfy some quanta conditions" [2].

De Broglie pointed out the appearance of integers in wave theory. He therefore saw "an indication in favor of the idea that, for electrons and other corpuscles, a wave-particle duality exists, as for photons and light waves" [2]. For him, it was obvious that a general synthesis needed to be done, applicable to light and matter. In 1924, de Broglie put forward the brilliant and revolutionary hypothesis that one could associate with a particle of momentum p a wave of frequency ν or wavelength λ, related to p by $p = h/\lambda$, where h is the Planck constant [3].

During his life, de Broglie's problem was to combine the two concepts, one statistical (wave), the other individual (particle). He tried, for example, to define a spatial-temporal model of particles of matter or light which involved hidden variables to explain their corpuscles and wave properties. He introduced two kinds of wave functions to solve the problem (double solution theory) [4]. In this work, he postulated that any solution φ of non-linear wave equations was

F. Frémont, *Young-Type Interferences with Electrons*, Springer Series on Atomic, Optical, and Plasma Physics 77, DOI 10.1007/978-3-642-38479-0_2,

accompanied by a solution u with a singularity (corpuscle) that had the same phase as φ. In fact, as shown by some of his colleagues, the combination of both solutions induced mathematical complications. Thus, one possible solution would be to say that, depending on circumstances, a particle behaves like either a corpuscle or a wave.

2.1.2 The First Evidence for Wave Behavior of Massive Particles

To prove wave-particle duality for electrons, "it was natural that the first application should be to the atom. No thought was given, after de Broglie's assumption, to electrons in free flight" [5]. Work began in 1919 by analyzing the energy of secondary electrons after they scattered on metal. It was discovered purely by accident that the intensity of elastic scattering varied with the orientation of the scattering crystal. The first to draw attention to this was Walter M. Elsasser, who pointed out in 1925 [6] that a demonstration of diffraction would establish the physical existence of electron waves. Elsasser wondered whether Davisson and Kunsman maxima and minima were diffraction phenomena similar to those produced by X-rays penetrating crystals [7]. He argued that anomalous peaks in the intensity of electrons could be evidence of electron diffraction. His publication was reviewed by Einstein who remained skeptical, but Elsasser's conclusions were found to be important for physicists such as Werner Heisenberg and Max von Laue.

The search for diffraction beams began at the end of 1926. A beam of electrons was directed against a crystal of nickel (Fig. 2.1).

A collector designed to accept only elastically scattered electrons could be moved in an arc of a circle around the crystal. The crystal itself could be rotated about the axis of the incident beam.

As shown in Fig. 2.2, the angular distribution for the intensity at a fixed azimuth of the crystal presents a maximum at a particular primary-beam voltage V (54 V in Fig. 2.2).

In Fig. 2.3, the wavelength derived from the angle of diffraction is represented as a function of $1/\sqrt{V}$ (points), and compared with the relation $\lambda = h/p$ (straight line). This remarkable agreement confirmed the wave behavior of electrons.

2.2 Interferences with Massive Particles

2.2.1 Interferences with Neutrons

In 1947, 15 years after the discovery of the neutron by James Chadwick, Enrico Fermi and Leona Marshall Libby systematically studied interferences produced by

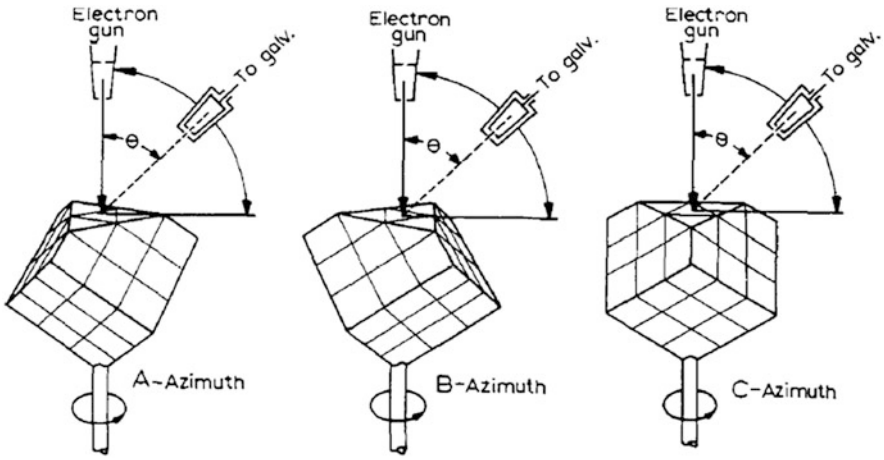

Fig. 2.1 Schematic view of the Davisson and Germer set-up, showing the arrangement of the primary electron beam, the crystal and the collector [5]. The crystal can be rotated around the azimuthal axis, and the detector can also be rotated in a plane

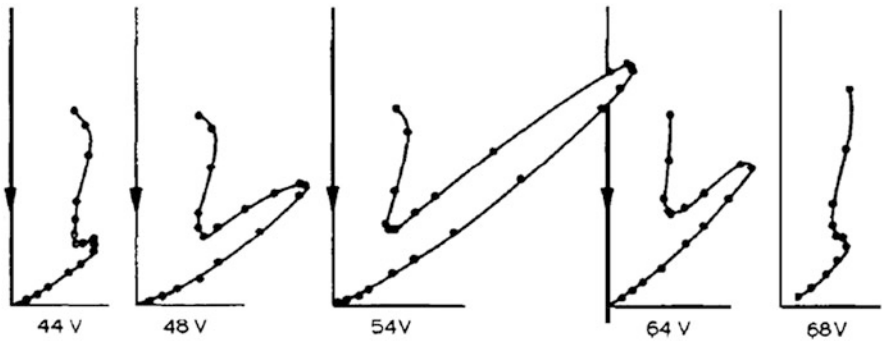

Fig. 2.2 Polar diagram showing intensity of elastic scattering in the A-azimuth as a function of the angle θ, for a series of primary-voltage beam [5]

slow neutrons scattering on various elements, such as Li, Be or C [8]. Their goal was to determine the phase change of the scattered neutron wave for a large number of elements. Their experimental set-up is schematically represented in Fig. 2.4. A beam of non-monochromatic thermal neutrons emerges from a hole containing a long collimator in the thermal column of the Argonne heavy-water pile. This beam falls on the 1, 0, 0 plane of a large CaF_2 crystal. Neutrons of energies satisfying the Bragg condition are reflected to form a beam that is used for investigating various crystal specimens. The beam contains a main component of neutrons of 0.15 nm wavelength, plus a small fraction of neutrons of energy four times as large due to the second-order reflection on the CaF_2 crystal. The second-order component is fairly insignificant. Therefore, one can consider the beam reflected on the calcite to

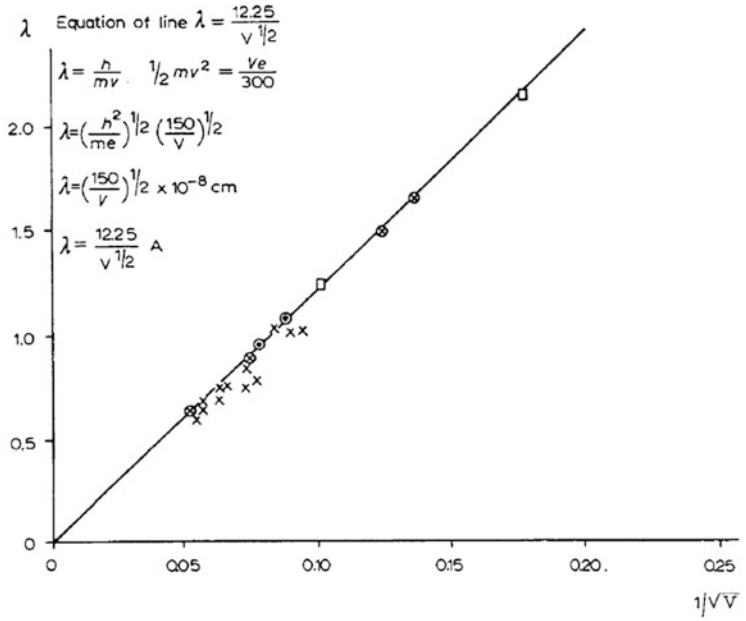

Fig. 2.3 Comparison between theoretical relation $\lambda = h/p$ and various experimental results (points) [5]

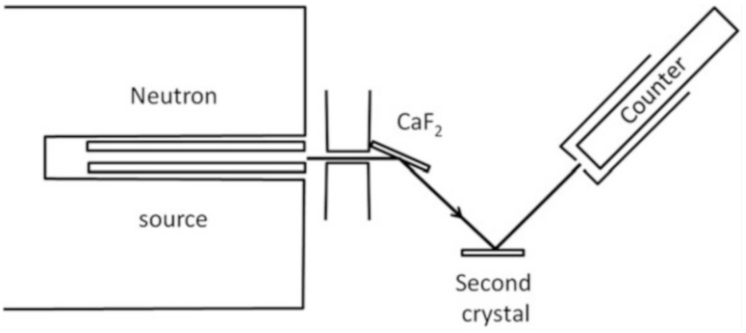

Fig. 2.4 Schematic view of the neutron interferometer set-up [8]

be approximately monochromatic. This monochromatic beam of neutrons falls on a plane of the second crystal, which is mounted on a rotating table. The neutrons undergo a second Bragg reflection, and are finally detected by a counter.

The scattering cross section σ is, in the first approximation, linked to the scattering length a by the relation

$$\sigma = \pi |a|^2 \tag{2.1}$$

A simple formula can be obtained in the case that scattering is due to the effect of a single resonant level. It is shown that a is proportional to the de Broglie wavelength λ associated with the energy of the primary neutrons. The total reflection of neutrons on mirrors is theoretically expected to occur at very small glancing angles. The limiting glancing angle is given, with very good approximation, by

$$\theta_o = \lambda\sqrt{Na/\pi} \tag{2.2}$$

where N is the atom density in the mirror. The agreement between the last formula and experimental angles is found to be good, with a relative uncertainty of less than 10 %, showing the wave behavior of the neutrons.

To observe maxima and minima in intensity, as observed for light, other set-ups were used. In 1974, a neutron interferometer was built (Fig. 2.5) with Si crystals as diffraction gratings [9]. The geometry of the device required the use of thermal neutrons to directly observe interference fringes. The first crystal played the role of beam separator. The second crystal recombined the transmitted and scattered beam, inducing interferences.

An aluminum plate, the angle of which was variable with respect to the neutron beam, was introduced to induce a path difference between the two beams. This path difference gave rise to interferences that could be detected. Figure 2.6 shows an example of the well-defined oscillations that are the signature of neutron interferences.

2.2.2 Interferences with Atoms

2.2.2.1 Double-Slit Experiment

Interferences with atoms were observed in the early 1990s [10]. The major problem was fringe spacing, i.e., the distance between bright and dark fringes. Using atoms at ambient temperature, the wavelength was less than one nanometer, and the fringes were therefore difficult to observe. On the contrary, if the atoms were cooled, their velocity decreased, and the wavelength increased. For example, for a velocity of the order of 100 m/s, the wavelength increased by a factor of ~100, inducing fringe spacing that could reach a few tenths of millimeters.

A supersonic jet of He crossed an interferometer, constituted by two slits separated by a distance of 8 μm (Fig. 2.7). Scattered atoms were detected by displacing a detector every 2 μm. The result of the detection is shown in Fig. 2.8 for a wavelength of 0.103 nm. Maxima and minima in intensity are visible, with a fringe spacing of 8.4 μm, in excellent agreement with theoretical predictions.

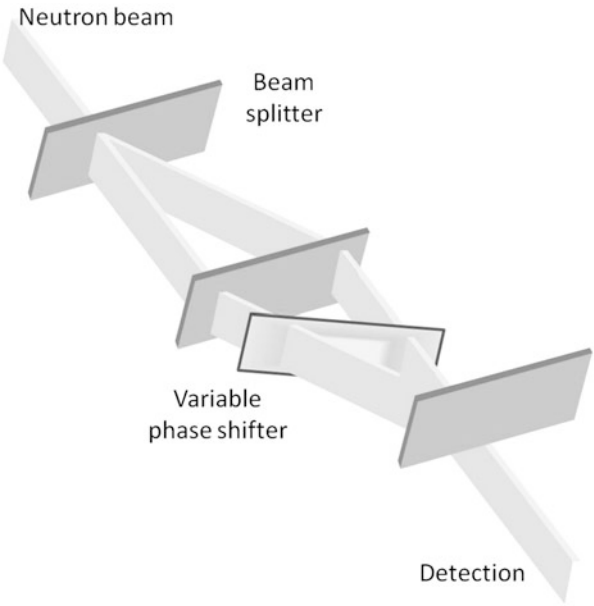

Fig. 2.5 Experimental set-up used to observe interferences produced by thermal neutrons

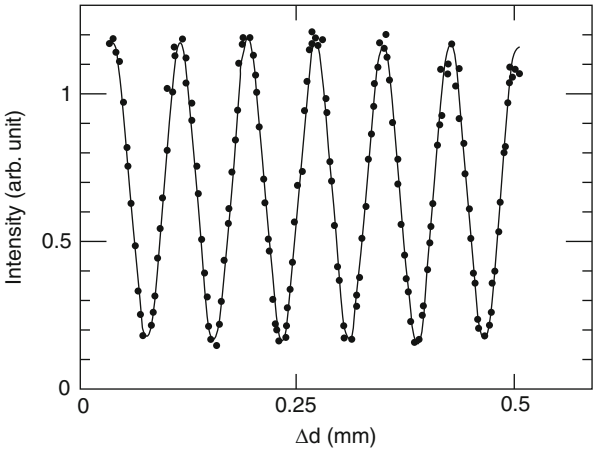

Fig. 2.6 Number of detected neutrons as a function of the path difference between scattered and transmitted beams. The oscillations are the signature of interferences

2.2.2.2 Three-Grating Experiment

To allow the largest interference signal for a given beam brightness, three-grating white-fringe geometry was used. In the experiment described in 1991 [11] for example, the atom beam consisted of a supersonic jet of sodium atoms (Fig. 2.9), giving rise to monochromaticity $\Delta v/v = 12$ %, with $v = 1{,}000$ m/s, inducing a wavelength of 16 pm. The diffraction gratings (G_1, G_2, and G3 in Fig. 2.9) consisted of arrays of slots in a silicon nitride membrane. The interferometer had three 400 nm-period gratings mounted apart on separate stages. The zeroth- and

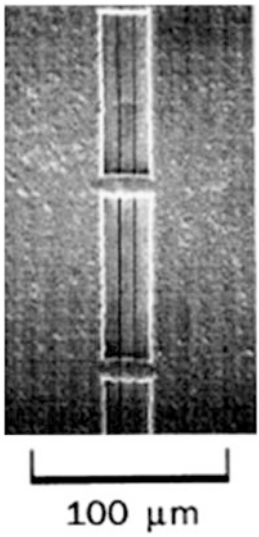

Fig. 2.7 Scanning-electron microscope picture of the transmission structure

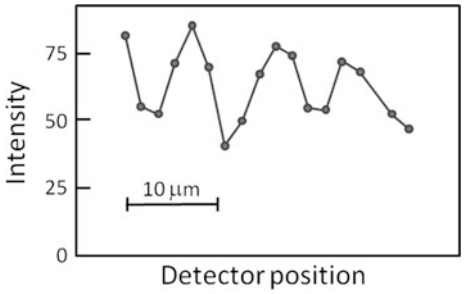

Fig. 2.8 Intensity profile in the detector plane as a function of the detector position

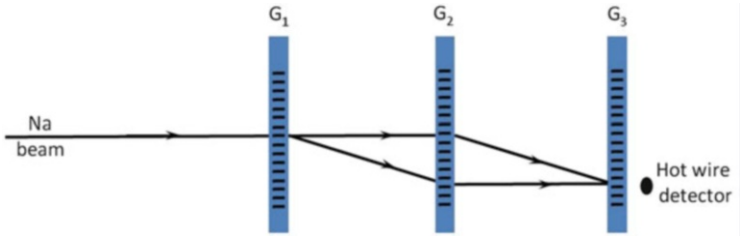

Fig. 2.9 Scheme of the three-grating interferometer [11]. The interferences are produced by a Na beam crossing the gratings G_1 and G_2

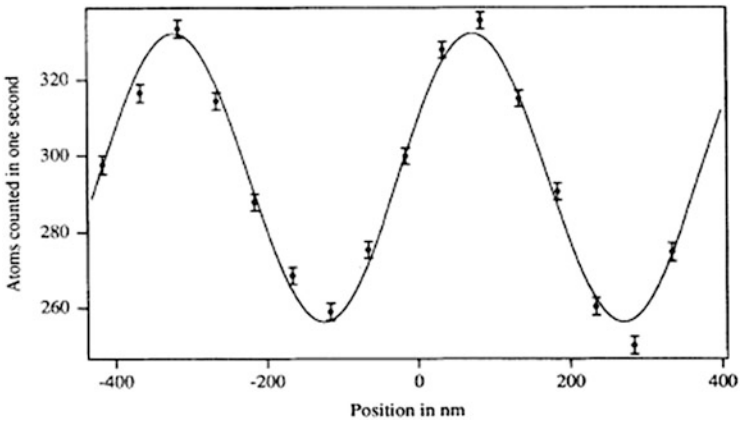

Fig. 2.10 Intensity as a function of the detector position. Experiment: *solid points*. Theory: *full curve*

first-order beams from the first grating struck the second one where they were diffracted in the positive and negative first orders to converge at the third grating. The first two gratings formed an interference pattern in the plane of the third grating, which acted as a mask to sample this pattern. A hot wire detector was moved in order to determine the number of counts as a function of the detector position.

The intensity, i.e., the number of scattered atoms, was thus recorded as a function of the detector. The experimental result is represented in Fig. 2.10 (solid points) as a function of the position. Well-defined oscillations can be observed, in very good agreement with the theoretical calculations (full curve).

2.2.2.3 Ramsey-Bordé Interferometry

The Ramsey-Bordé interferometer is analogous to the Mach-Zehnder interferometer for light (cf. Chap. 1, Sect. 1.1.6.2) which uses separators and mirrors. The principle of the beam splitter (separator) is the following. Suppose that one atom has two ground state hyperfine sub-levels $\left|\overrightarrow{k}, g_1, 0\right\rangle$ and $\left|\overrightarrow{K}, g_2, 0\right\rangle$, where 0 is the number of transferred photons (Fig. 2.11) and $\overrightarrow{k}$ and $\overrightarrow{K}$ are the atom momenta associated with each state [12].

The atom absorbs one photon of energy $\hbar\omega_1$ and emits by stimulated emission a photon of energy $\hbar\omega_2$. Thus the atom can be in the ground state $\left|\overrightarrow{K}, g_2, 0\right\rangle$ with a given probability. The absorption and emission of the two photons is accompanied by a change in the momentum $\overrightarrow{k}$, which is the sum of the two momenta $\overrightarrow{k_1}$ and $\overrightarrow{k_2}$ due to each photon (Fig. 2.12).

The Ramsey-Bordé interferometer is composed of several beam splitters similar to the one described above. An example is given in Fig. 2.13 [13]. The probability of absorption and stimulated emission is chosen to be 50 % in each interaction zone

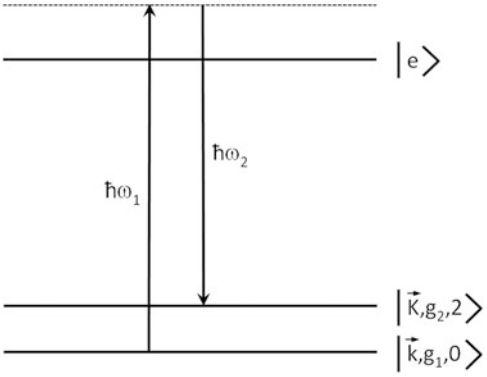

Fig. 2.11 Principle of atom diffraction using a Raman process [12]. The atom absorbs a photon of energy $\hbar\omega_1$, and emits a photon of energy $\hbar\omega_2$ by stimulated emission

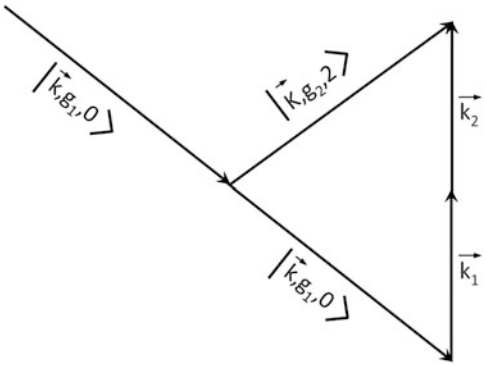

Fig. 2.12 Momentum conservation during photon absorption and emission. The initial and final momenta are $\overrightarrow{k}$ and $\overrightarrow{K}$, respectively [12]

by applying the proper laser intensity and interaction time. The first interaction (first arrow in Fig. 2.13), for example, produces the superposition $1/\sqrt{2}\left(\left|\overrightarrow{k}, g_1, 0\right\rangle + \left|\overrightarrow{k} + \overrightarrow{k_1}, e, +1\right\rangle\right)$, with a phase depending on the laser.

Two classes of interferometers can be defined [14].

- In open interferometers (e.g., Young's double-slit interferometer), a single beam divider produces a coherent superposition of waves. The interference pattern which results from the superposition of several outgoing wavefronts is explored directly by moving a detector in space or in time.
- In a closed interferometer, the outgoing waves are re-superposed by a second beam splitter. The interference pattern is observed by scanning the phase difference between the two beam splitters.

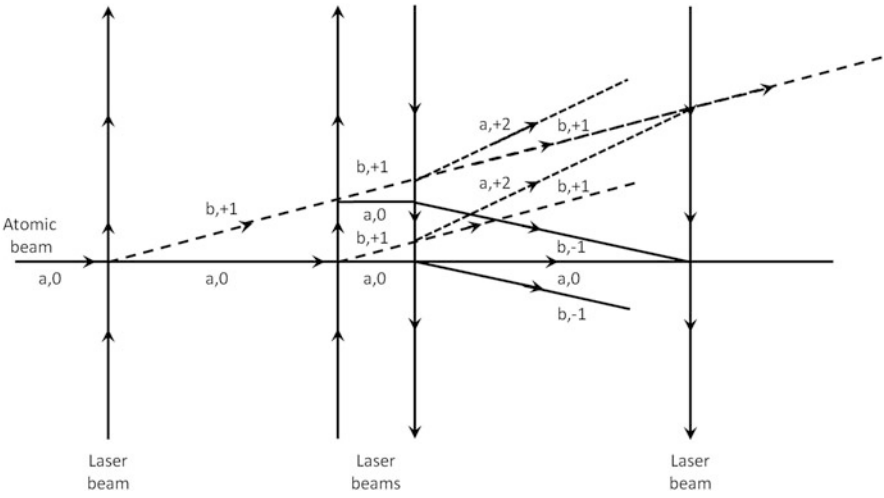

Fig. 2.13 Ramsey-Bordé type interferometer. The atom is initially in state *a,0*. The use of lasers can produce intermediate or final states labeled *b,+1*, *b,−1* and *a,+2*

The Ramsey-Bordé interferometer is particularly used for high-precision measurements of gravity, polarizability measurements, the determination of the effects of a magnetic field, and the analysis of inertial effects.

2.2.3 Interferences with Small Molecules

Since interferometry is applied to atoms, it is also well suited for small molecules. In 2000, for example, interference pattern was studied for diatomic molecules He_2. In this molecule's fundamental state, its atoms are separated by ~5 nm, which is much greater than for most molecules. These molecules are produced from an atomic source (Fig. 2.14) and then separated by beam diffraction.

The grating consists of slits of a width of 500 nm, separated by 500 nm. The trajectories of the diffracted elements depend on their mass, so that these elements can be analyzed by mass spectroscopy. Figure 2.15 shows a typical spectrum obtained after diffraction, for temperatures T of the source varying between 4.5 and 65 K. One can see first that the dimer production is weak (~1,000 times less than that of He atoms). The angular distribution reveals series of maxima and minima in intensity. When T decreases, the energy decreases, so that the wavelength and thus the fringe spacing increase.

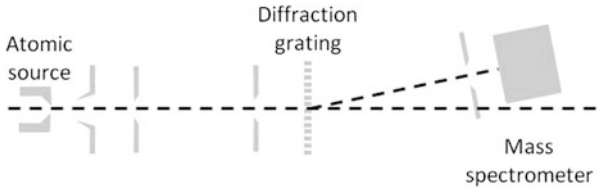

Fig. 2.14 An atomic source produces He atoms and He_2 dimers. The dimers are separated by diffraction and analyzed using a mass spectrometer

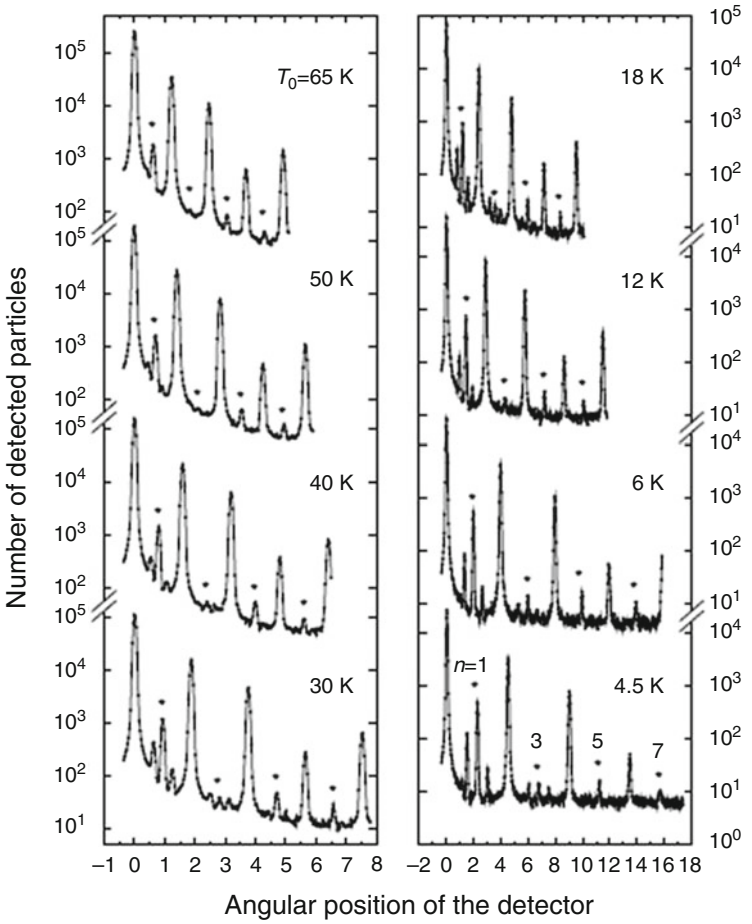

Fig. 2.15 Spectra of He atoms and dimers of He obtained after diffraction for several temperatures of the atomic source. The positions of the dimers are indicated by points

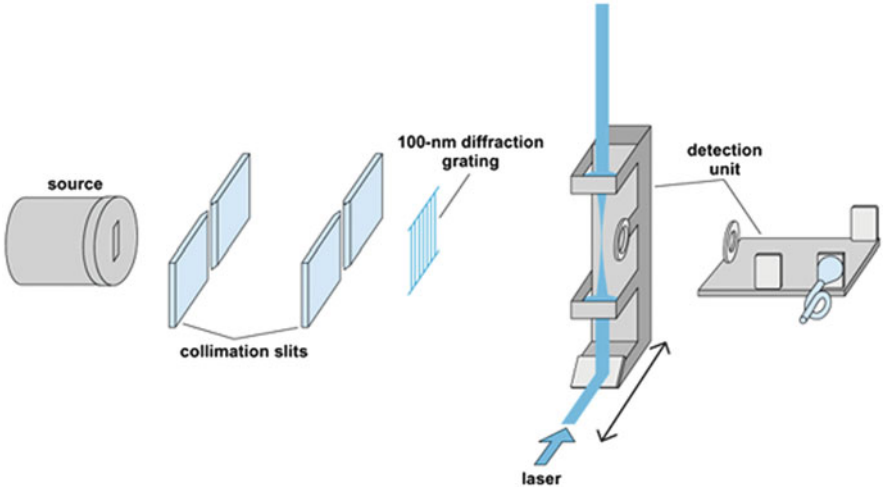

Fig. 2.16 Experimental set-up for C_{60} interferences. The source produces the fullerenes that are deviated by a grating. A laser induces a phase and the products are finally detected

2.2.4 Interferences with Large Molecules and Clusters

We know that the wave nature of particles is increasingly difficult to observe as their mass increases, because the de Broglie wavelength decreases strongly. However, 10 years ago, the wave nature of fullerenes was demonstrated [15, 16]. To observe the interference pattern, the experimental set-up was similar to that used for atoms [15]. The fullerenes were heated, and the velocity selected (Fig. 2.16). The most probable velocity was of the order of 200 m/s, inducing a wavelength of ~3 pm. The fullerenes were then passed through a grating, consisting of slits of a width of 50 nm and separated by a distance of 100 nm. The fringe spacing was thus ~34 μm. The diffracted atoms were then ionized using a laser, and the resulting ions accelerated and directed towards a conversion electrode.

Figure 2.17 presents the typical results for the intensity. On the bottom, the profile beam is given without grating. With the grating (top of the figure), the diffraction pattern is observed (open circles). The essential features of the interference pattern can be understood using standard Kirchhoff diffraction theory for a grating with a period of 100 nm, taking into account both the finite width of the collimation and the experimentally determined velocity distribution. The parameters in the fit were the width of the collimation, the gap width s_0 of a single slit opening, the effective beam width of the detection laser, and an overall scaling factor. This model, which assumes all grating slits to be perfect and identical, reproduces the central peak of the interference pattern very well, as shown in Fig. 2.17a.

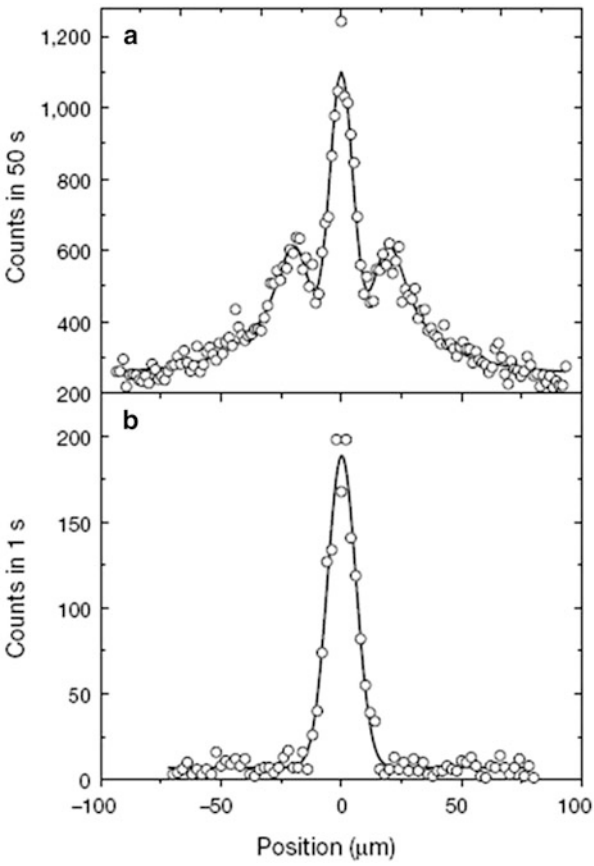

Fig. 2.17 Interference pattern produced by C_{60} molecules. (**a**) Experimental recording (*open circles*) and fit using Kirchhoff diffraction theory (*continuous line*). The expected zeroth- and first-order maxima can be clearly seen. (**b**) The molecular beam profile without the grating in the path of the molecules

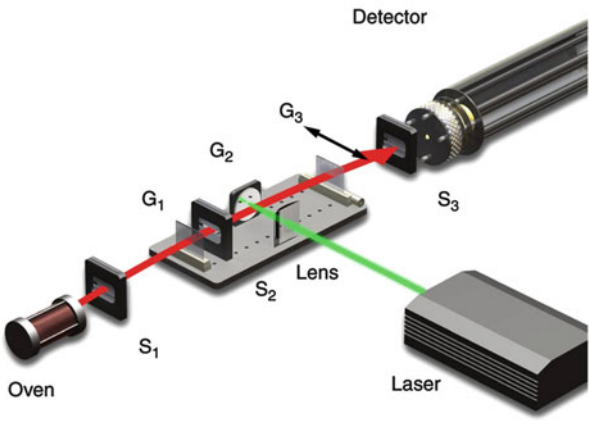

Fig. 2.18 Experimental device devoted to interference observation for large organic molecules [17]

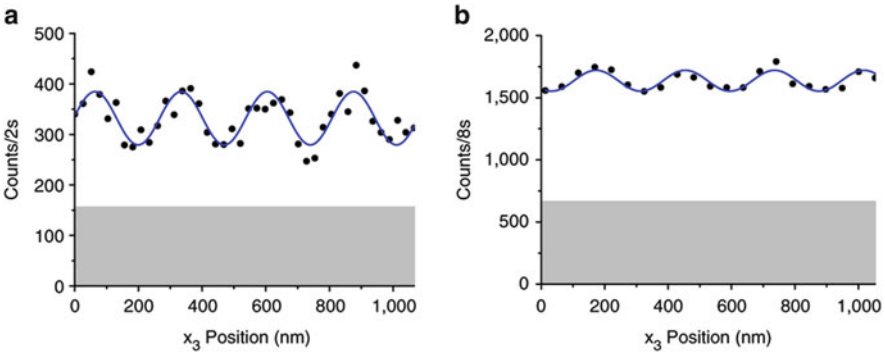

Fig. 2.19 Quantum interference is observed for two species, as a function of the third grating position. (**a**) perfluoroalkylated nanospheres $C_{60}(C_{12}F_{25})_8$. (**b**) $C_{60}(C_{12}F_{25})_{10}$. The *shaded area* indicates the detector dark rate

The wave nature of very massive organic molecules was demonstrated in 2011 [17]. An effusive source emitted molecules of e.g., $C_{60}(C_{12}F_{25})_8$ and $C_{44}H_{30}N_4$ whose masses were greater than 600 amu. The velocity of the molecules was selected through a sequence of three slits (Fig. 2.18).

Each slit of G_1 imposed a constraint onto the transverse molecular position that led to a momentum uncertainty. The latter turned into a growing delocalization and transverse coherence of the matter wave with increasing distance from G_1. The second grating G_2 was a laser light wave with a wavelength of $\lambda = 532$ nm. The interaction between the electric laser light field and the molecular optical polarizability created a sinusoidal potential, which phase-modulated the incident matter waves. The molecular nanostructure was sampled by scanning a third grating G_3 across the molecular beam while counting the number of the transmitted particles in a quadrupole mass spectrometer (QMS).

The interference fringes can be observed with a very good contrast, as shown in Fig. 2.19 for two species.

2.2.5 *Interferences with Bose-Einstein Condensates*

The indistinguishability of identical particles has important consequences. At very low temperatures, bosons can occupy the same state, giving rise to Bose-Einstein (BE) condensates. To obtain BE condensates, one method has been to employ a combination of laser cooling and evaporation cooling to produce dense, cold atomic clouds (Fig. 2.20).

Two years after the first creation of BE condensates, an experiment was performed to observe the interference pattern of two condensates of Na [18]. After letting the

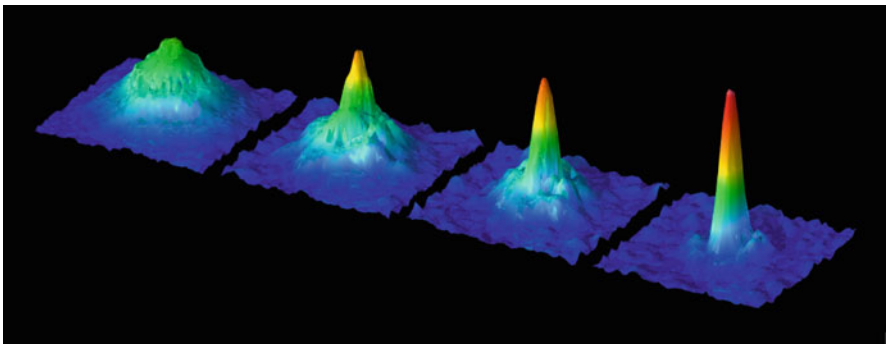

Fig. 2.20 Atoms of Rb (*left-hand side*) are cooled in a double magneto-optical trap. The atoms are laser-cooled to a temperature of ~0.03 K, and then transferred to a magneto-optical trap where they are cooled by radio-frequency evaporation. After ~5 s, a temperature of 500 nK is reached

Fig. 2.21 Interference pattern of two expanding condensates observed after 40 ms time of flight [18]

condensates expand and overlap, interference between them was observed, with high-contrast fringes. The observation of interference (Fig. 2.21) demonstrated that BE condensates were coherent, i.e., they behaved like lasers.

References

1. Bohr, N.: On the constitution of atoms and molecules. Philos. Mag. **26**, 1 (1913)
2. de Broglie, L.: La physique quantique reste-t-elle indéterministe?, Revue d'histoire des sciences et de leurs applications, tome 5, no4 (1952)
3. de Broglie, L.: Recherche sur la théorie des quanta, Thèse, Paris (1924)

4. de Broglie, L.: *La* Mécanique ondulatoire et la structure atomique de la matière et du rayonnement. J. Phys. Paris, série VI, t. VIII 225, 15–31 (1927)
5. Davisson, C.J.: The discovery of electron waves. Nobel lecture 1937, Physics 1922–1941, Elsevier Publishing Company, Amsterdam (1965)
6. Elsasser, W.: Bemerkungen zur Quantenmechanik frier Elektronen. Naturwissenschafter **13**, 711 (1925)
7. Davisson, C.J., Kunsman, C.H.: Scattering of low speed electrons by platinum and magnesium. Phys. Rev. **22**, 242 (1923)
8. Fermi, E., Marshall, L.: Interference phenomena of slow neutrons. Phys. Rev. **75**, 666 (1947)
9. Rauch, H., Treimer, W., Bonse, U.: Test of a single crystal neutron interferometer. Phys. Lett. A **47**, 369 (1974)
10. Carnal, O., Mlynek, J.: Young's double-slit experiment with atoms: a simple atom interferometer. Phys. Rev. Lett. **66**, 2689 (1991)
11. Keith, D.W., et al.: An interferometer for atoms. Phys. Rev. Lett. **66**, 2693 (1991)
12. Miffre, A., et al.: Atom interferometry. Phys. Scr. **74**, C15 (2006)
13. Bordé, C.J.: Atomic interferometry with internal state labeling. Phys. Lett. A **140**, 10 (1989)
14. Baudon, J., Mathevet, R., Robert, J.: Atomic interferometry. J. Phys. B **32**, R173 (1999)
15. Arndt, M., et al.: Wave-particle duality of C_{60} molecules. Nature **401**, 680 (1999)
16. Arndt, M., et al.: High contrast interference with C_{60} and C_{70} molecules. C. R. Acad. Sci. Paris, t.2, Série 4 581 (2001)
17. Gerlich, S., et al.: Quantum interference of large organic molecules. Nat. Com. **2**, 263 (2011)
18. Andrews, M.R., et al.: Observation of interference between two Bose condensates. Science **173**, 637 (1997)

http://www.springer.com/978-3-642-38479-0

Young-Type Interferences with Electrons
Basics and Theoretical Challenges in Molecular Collision Systems
Frémont, F.
2014, XI, 227 p.,
ISBN: 978-3-642-38479-0